

considerable flexibility in regulating the presentation of lipid antigens, will be critical to improve the rational design of lipid vaccines and adjuvants.

References and Notes

- D. B. Moody, S. A. Porcelli, *Nat. Rev. Immunol.* **3**, 11 (2003).
- A. Bendelac *et al.*, *Science* **268**, 863 (1995).
- T. Kawano *et al.*, *Science* **278**, 1626 (1997).
- D. I. Godfrey, K. J. Hammond, L. D. Poulton, M. J. Smyth, A. G. Baxter, *Immunol. Today* **21**, 573 (2000).
- A. Bendelac, M. Bonneville, J. F. Kearney, *Nat. Rev. Immunol.* **1**, 177 (2001).
- D. B. Moody *et al.*, *J. Exp. Med.* **192**, 965 (2000).
- M. Sugita *et al.*, *Science* **273**, 349 (1996).
- R. M. Jackman *et al.*, *Immunity* **8**, 341 (1998).
- Y. H. Chiu *et al.*, *J. Exp. Med.* **189**, 103 (1999).
- Y. H. Chiu *et al.*, *Nat. Immunol.* **3**, 55 (2002).
- A. Shamshiev *et al.*, *Immunity* **13**, 255 (2000).
- D. B. Moody *et al.*, *Nat. Immunol.* **3**, 435 (2002).
- M. Sugita *et al.*, *Immunity* **16**, 697 (2002).
- V. Briken, R. M. Jackman, S. Dasgupta, S. Hoening, S. A. Porcelli, *EMBO J.* **21**, 825 (2002).
- J. Jayawardena-Wolf, K. Benlagha, Y. H. Chiu, R. Mehr, A. Bendelac, *Immunity* **15**, 897 (2001).
- S. J. Kang, P. Cresswell, *EMBO J.* **21**, 1650 (2002).
- D. G. Rueckert, K. Schmidt, *Chem. Phys. Lipids* **56**, 1 (1990).
- K. Sandhoff, T. Kolter, G. Van Echten-Deckert, *Ann. N.Y. Acad. Sci.* **845**, 139 (1998).
- C. S. Wright, Q. Zhao, F. Rastinejad, *J. Mol. Biol.* **331**, 951 (2003).
- V. E. Ahn, K. F. Faull, J. P. Whitelegge, A. L. Fuharty, G. G. Prive, *Proc. Natl. Acad. Sci. U.S.A.* **100**, 38 (2003).
- N. Fujita *et al.*, *Hum. Mol. Genet.* **5**, 711 (1996).
- D. Zhou *et al.*, unpublished observations.
- A. Bendelac, M. N. Rivera, S.-H. Park, J. H. Roark, *Annu. Rev. Immunol.* **15**, 535 (1997).
- T. I. Prigozy *et al.*, *Science* **291**, 664 (2001).
- C. V. Harding, D. S. Collins, J. W. Slot, H. J. Geuze, E. R. Unanue, *Cell* **64**, 393 (1991).
- T. Ohshima *et al.*, *Proc. Natl. Acad. Sci. U.S.A.* **94**, 2540 (1997).
- N. Sakai *et al.*, *J. Neurochem.* **66**, 1118 (1996).
- C. Vogler *et al.*, *Pediatr. Res.* **49**, 342 (2001).
- Q. Zhao, C. R. Morales, *J. Biol. Chem.* **275**, 24829 (2000).
- C. Cantu III, K. Benlagha, P. B. Savage, A. Bendelac, L. Teyton, *J. Immunol.* **170**, 4673 (2003).
- L. K. Denzin, P. Cresswell, *Cell* **82**, 155 (1995).
- X. Qi, T. Leonova, G. A. Grabowski, *J. Biol. Chem.* **269**, 16746 (1994).
- Y. Y. Wu *et al.*, *J. Biol. Chem.* **269**, 16276 (1994).
- R. Kase *et al.*, *FEBS Lett.* **393**, 74 (1996).
- We thank R. Brown, E. Berger, K. Sandhoff, and B. Jabri for helpful suggestions and E. Rosloniec and A. Rudensky for I-A^b- and I-A^d-restricted T cell hybridomas. Supported by NIH grants (PO1 AI53725 to P.S., A.B., and L.T. and AI50867 and AI38339 to A.B.) and the Cancer Research Institute (D.Z. and Y.S.).

Supporting Online Material

www.sciencemag.org/cgi/content/full/1092009/DC1

Materials and Methods

Figs. S1 to S4

29 September 2003; accepted 21 November 2003

Published online 18 December 2003;

10.1126/science.1092009

Include this information when citing this paper.

T Cell Activation by Lipopeptide Antigens

D. Branch Moody,^{1*} David C. Young,^{1,2} Tan-Yun Cheng,¹ Jean-Pierre Rosat,¹ Carme Roura-mir,¹ Peter B. O'Connor,² Dirk M. Zajonc,⁵ Andrew Walz,³ Marvin J. Miller,³ Steven B. Levery,⁴ Ian A. Wilson,^{5,6} Catherine E. Costello,² Michael B. Brenner¹

Unlike major histocompatibility proteins, which bind peptides, CD1 proteins display lipid antigens to T cells. Here, we report that CD1a presents a family of previously unknown lipopeptides from *Mycobacterium tuberculosis*, named didehydroxymycobactins because of their structural relation to mycobactin siderophores. T cell activation was mediated by the $\alpha\beta$ T cell receptors and was specific for structure of the acyl and peptidic components of these antigens. These studies identify a means of intracellular pathogen detection and identify lipopeptides as a biochemical class of antigens for T cells, which, like conventional peptides, have a potential for marked structural diversity.

Dendritic cells (DCs) play a central role in stimulating T lymphocyte responses (1). Myeloid DCs and Langerhans cells of the skin can be identified in tissues on the basis of their abundant and specific expression of the major histocompatibility complex (MHC) class I–like protein CD1a, among other mark-

ers (2, 3). The function of CD1a involves the presentation of self and foreign antigens to T cells (4–6). The general molecular mechanism of antigen presentation by CD1 involves insertion of the alkyl chains of amphipathic lipids into a deep hydrophobic groove formed by the $\alpha 1$ and $\alpha 2$ domains of the CD1 heavy chain. This positions carbohydrate or other hydrophilic elements of the antigen on the outer surface of CD1, where they can directly contact T cell receptors (TCR) (7–9). CD1a-restricted T cells recognize mycobacteria-infected cells and have antibacterial effects, suggesting a possible role in host defense (5, 10). In addition, CD1a is normally expressed on DCs early in their maturation program, so CD1a-mediated T cell activation events that occur at the surface of infected DCs are well positioned to influence DC maturation (2, 11). However, the molecular structures of foreign antigens presented by CD1a have not been determined.

To identify candidate antigens presented by CD1a, TCR α and β chains from the CD1a-restricted and mycobacteria-specific T cell line CD8-2 were cloned and transfected into J.RT3-T3.5 T lymphoblastoid cells to generate a reporter cell line, J.RT3.CD8-2 (5). Along with untransfected J.RT3 cells, this cell line was used to screen for antigens in chromatographic fractions generated from complex mixtures of compounds found in *M. tuberculosis* cell walls. Antigenic factors capable of J.RT3.CD8-2 activation were efficiently extracted from whole mycobacteria by using chloroform:methanol (2:1), suggesting that the antigens were lipids, which were not covalently bound to the arabinogalactan complex of the mycobacterial cell wall (12). Elution of the stimulatory lipids from silica columns in polar solvents, such as methanol, indicated that the antigens displayed characteristics of polar lipids. Purification by high-performance liquid chromatography (HPLC) led to the isolation of a fraction that contained a set of structurally related compounds, which, by mass spectrometry analysis, yielded a prominent $[M+H]^+$ ion at mass/charge ratio (m/z) 838.5. This antigenic compound was initially named 838 on the basis of its nominal mass.

C1R lymphoblastoid cells transfected with human CD1a, but not CD1b, CD1c, or CD1d, were able to present 838 to J.RT3.CD8-2 (Fig. 1A). T cell activation was not seen with other known CD1-presented lipid antigens such as mycolic acid, glucose monomycolate, or mannosyl phosphoisoprenoids (Fig. 1B). Also, 838 did not activate polyclonal T cells or J.RT3 transfectants expressing TCRs that are specific for lipid antigens presented by CD1b or CD1c (Fig. 1B) (13–15). Together, these studies indicated that 838 did not function as a mitogen, but instead activated cells through CD1a-restricted

¹Division of Rheumatology, Immunology and Allergy, Brigham and Women's Hospital and Harvard Medical School, Smith Building Room 514, 1 Jimmy Fund Way, Boston, MA 02115, USA. ²Mass Spectrometry Resource, Boston University School of Medicine, 715 Albany Street, R806, Boston, MA 02115, USA. ³Department of Chemistry and Biochemistry, University of Notre Dame, 251 Nieuwland Science Hall, Notre Dame, IN 46556–5670, USA. ⁴Department of Chemistry, University of New Hampshire, Durham, NH 02834, USA. ⁵Department of Molecular Biology and the ⁶Skaggs Institute for Chemical Biology, The Scripps Research Institute, 10550 North Torrey Pines Road, La Jolla, CA 92037, USA.

*To whom correspondence should be addressed. E-mail: bmoody@rics.bwh.harvard.edu

recognition mediated by clonally variable regions of the TCR α and β chains.

Further insights into the molecular composition of 838 were obtained through high-resolution mass measurements. Fourier transform ion cyclotron resonance mass spectrometry (FTICR-MS) demonstrated the $[M+H]^+$ to be m/z 838.5684, matching the value calculated for $C_{47}H_{76}N_5O_8$ (838.5688) (table S1). Tandem mass spectrometry (MS/MS) yielded product ions at m/z 642 and m/z 197, which were each 16 u (the mass of oxygen) smaller than the previously described mycobactin acid and cobactin fragments of mycobactin, a known mycobacterial lipopeptide with iron-scavenging properties (16, 17). Therefore, we named the antigen dihydroxymycobactin (DDM-838). Identification of MS/MS products at m/z 727 and 84 indicated that the hydroxyls found in mycobactin were substituted by lysines in the proposed structure for DDM (17). The presence of lysine in DDM was confirmed by gas chromatography–mass spectrometry (GC-MS) of acid hydrolysis products. Unexpectedly, GC-MS detected an uncommon amino acid, α -methyl serine, instead of serine and threonine, which are present in most mycobacterial mycobactins (12, 16, 18). The identity of α -methyl serine as a component of DDM was confirmed by the nuclear magnetic resonance (NMR) spectrum of DDM (Fig. 2C), as well as by differences in the MS/MS spectra of *M. tuberculosis* DDM compared with synthetic DDM homologs that contained threonine (DDM-thr) (19). These studies establish the structure of the CD1a-presented antigens produced by *M. tuberculosis* and show that they conform to a general structure in Fig. 2B, which is composed of salicylic acid, α -methyl serine, acylated lysine, hydroxybutyrate, and cyclized lysine (Fig. 2B).

Dihydroxymycobactin most likely functions as an intermediate in mycobactin synthesis. The mycobactin locus in *M. tuberculosis* encodes mycobactin synthase genes, MbtA to MbtJ, which function as a nonribosomal peptide synthesis pathway (20). Previously proposed schemes of mycobactin biosynthesis have emphasized a likely role of MbtA, MbtB, MbtC, MbtD, MbtE, and MbtF in activating the salicylic moiety and synthesizing the peptide (Fig. 2D) (19, 21, 22). The final steps in mycobactin synthesis were thought to involve peptide termination by intramolecular attack of the lysine side chain on its carboxy terminus and by acylation and hydroxylation of the two lysine residues (Fig. 2D). Although the precise order in which these terminal steps occur is not known, the discovery of DDM clarifies the order by suggesting that the lysines are incorporated into the peptide and subsequently hydroxylated to yield mycobactins (Fig. 2D). The two hydroxyl moieties, which are present in myco-

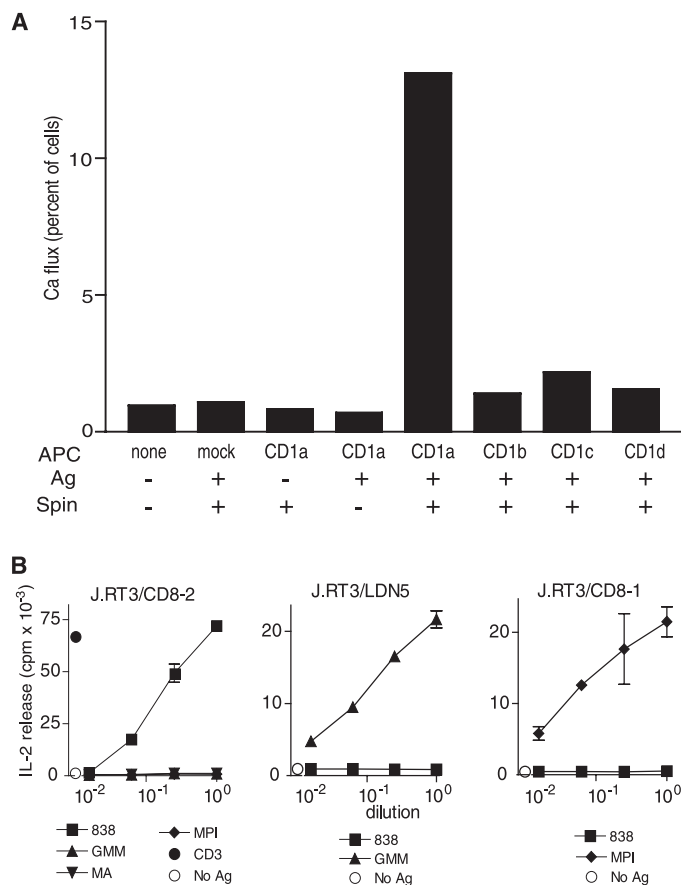
bactin but absent in DDM, form two sites, which mediate high-affinity ($\sim 10^{-26}$ M) binding to iron (16). Consistent with the predicted roles of these hydroxyl groups in iron binding, we found that mycobactin was detected in the iron-bound form solely as $[M+Fe-2H]^+$ at m/z 923.5, whereas DDM was detected solely in the unbound form as a proton adduct of m/z 838.6.

During infection, bacteria must obtain iron from host stores to support a variety of reduction-oxidation reactions necessary for normal bacterial metabolism. Bacteria scavenge iron by producing siderophores, which bind iron with high affinity at or near the bacteria-host interface and deliver iron to the bacterium (23). Mycobacteria produce mycobactin and related siderophores, whose synthesis is triggered by derepression of mycobactin synthase genes during growth in low-iron conditions (24). This process normally occurs during growth in host cells and is known to be necessary for *M. tuberculosis* survival within human macrophages (25). These considerations suggested that DDM might be synthesized as an intermediate in mycobactin produc-

tion during intracellular infection. We found that DDM-specific T cell activation occurs efficiently in cells infected with five bacteria per cell of *M. tuberculosis*, whereas *M. tuberculosis* grown in complete medium requires the equivalent of 10^{11} bacteria to produce detectable levels of DDM, and in some cases does not produce DDM at all (Fig. 3A). Because CD1a-restricted T cells are able to kill mycobacteria-infected cells (26), CD1a presentation of DDM may represent an early warning system for intracellular pathogen recognition, whereby bacterial metabolites, which are necessary for adapting to intracellular growth, result in T cell activation.

To analyze more precisely the role of DDM structure in mediating T cell activation, we used HPLC to isolate several natural lipopeptides from *M. tuberculosis*. In addition to DDM-838 (Fig. 3B, peak E), *M. tuberculosis* produced a series of structurally related compounds (peaks A to D and F). Although the abundance, as determined by ultraviolet absorbance, correlated well with the measured T cell response for some compounds (Fig. 3B, peaks A, C, D, and

Fig. 1. T cell activation by antigen 838 is CD1a and TCR dependent. **(A)** C1R B lymphoblastoid cells transfected with cDNA constructs encoding the indicated human CD1 isoform or an empty vector (mock) were coincubated overnight with *M. tuberculosis* lipid fractions containing the 838 antigen. After adding J. RT3.CD8-2 cells at a 1:1 ratio and subjecting cells to a 1 min centrifugation (spin) to initiate cell contact, we measured calcium flux by flow cytometry of J.RT3 T cells labeled with calcium-sensitive fluorescent dyes Fura-red and Fluo 4 (32). **(B)** J.RT3 T lymphoblastoid cells were transfected with the TCR α and β chains cloned from the human T cell lines CD8-2, LDN5 (CD1b-restricted and glucose monomycolate specific), or CD8-1 (CD1c-restricted and mannosyl phosphoisoprenoid-specific) (14, 15, 33). Using monocyte-derived dendritic cells as antigen-presenting cells, we added monoclonal antibody to CD3 (OKT3) (30 ng/ml) or lipid antigens at or above concentrations that were previously known to be activating for T cells. These antigens were 838 (1 μ M), mycolic acid (MA) (30 μ M), glucose monomycolate (GMM) (30 μ M), or mannosyl phosphoisoprenoid (MPI) (one-tenth dilution of fraction purified by 2D thin-layer chromatography). Interleukin-2 (IL-2) release was measured with the HT-2 bioassay (32).



E), others showed weak (peak F) or no (peak B) ability to activate T cells. Compounds in peaks A, B, E, and F were purified and found to have nominal masses of 810, 812, 838, and 840, respectively. MS/MS demonstrated that DDM-838 bore a C20:1 fatty acid, whereas DDM-840, DDM-812, and DDM-810 contained peptides of equal masses but were substituted with differing fatty acids, C20:0, C18:0, and C18:1, respectively (Figs. 2B and 3C). A comparison of NMR spectra for DDM-838 and DDM-840 indicated that the unsaturation of the fatty acyl component of DDM-838 was at the C₂₋₃ position, likely in a cis conformation (Fig. 2C). Whereas DDM-838 gave the most potent T cell response, homologous lipopeptides that had shorter or saturated fatty acids were substantially less stimulatory (Fig. 3C). Natu-

ral mycobactins were not recognized, suggesting that the hydroxylation of the lysine residues prevents T cell recognition (Fig. 3C). Also, lipid fractions containing mycobactin acid, which corresponds to a truncated lipopeptide lacking the butyric acid-lysine moiety (Fig. 2B, *m/z* 642 fragment), were recognized weakly or not at all (12). Thus, the T cell response was specific for the structure of the peptide and the length and saturation state of the fatty acyl chain.

These studies identify lipopeptides as a biochemical class of antigens for T cells, which share structural features of MHC-presented peptides and CD1-presented glycolipids. The crystal structure of CD1a shows that the antigen-binding groove is composed of an F' pocket, which is wide, largely exposed, and broadly contiguous with the predicted TCR contact surface (8). The A' pocket

is largely hydrophobic, with no obvious polar groups that could hydrogen bond with the peptidic portion of DDM in the way that MHC molecules bind to peptides. Also, the A' pocket is narrow and terminates deep within the CD1a structure, so that it may act as a ruler to select out acyl chains of a particular length. A molecular model shows that the C20:1 fatty acyl moiety could fit well within the A' pocket, positioning the peptide backbone at the broad junction of the A' and F' pockets, so that it would be available for contact with the TCR (Fig. 3D). Although the orientation of the peptidic moiety cannot be predicted precisely, the only polar residues in the binding groove are located at the A'-F' junction, so it seems plausible that the same residues that are known to bind the sulfogalactosyl moiety of sulfatide also hydrogen bond with the peptidic portion of DDM (8).

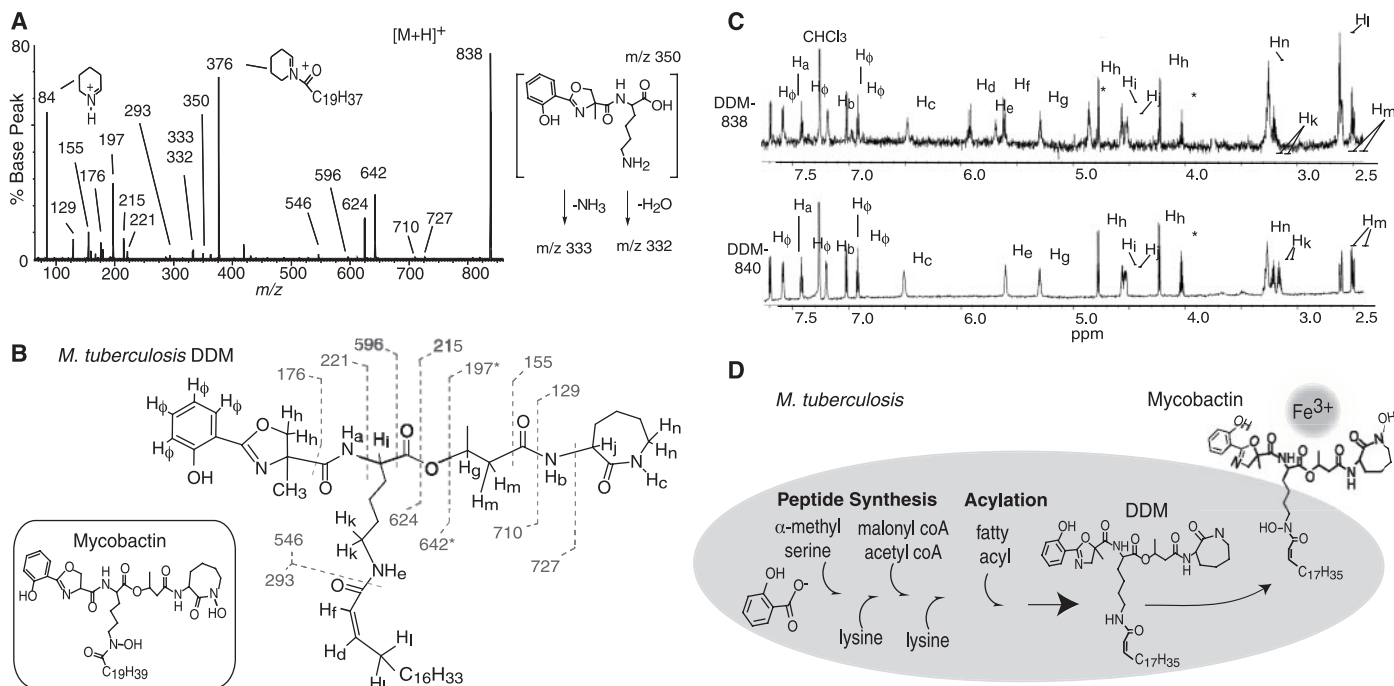


Fig. 2. Structure of the CD1a-presented antigen, DDM-838. **(A and B)** The DDM structure was deduced from the MS/MS spectrum of $[M+H]^+$ *m/z* 838. Major complementary ions derived from DDM-838 were present at *m/z* 624 and *m/z* 215, which differed by 16 u from mycobactin acid and cobactin fragments of mycobactin (inset) (16, 19). Simple one-bond fragmentations are indicated by dashed lines and assume hydrogen transfer to nitrogen and oxygen during amide and ester cleavage. Multistep fragmentations explain the ions at *m/z* 376, *m/z* 350, *m/z* 333, *m/z* 332, and *m/z* 84. **(C)** Downfield regions of one-dimensional proton NMR spectra of DMM-838 (upper) and DDM-840 (lower) show resonances that are assigned as aromatic (H_ϕ) or other protons (H_a -n), as denoted in (B). The olefinic protons H_d and H_f are present in DDM-838, but not in DDM 840, and are coupled to each other with a J constant of 12.1 Hz. This is consistent with a double bond, which is likely present at C₂₋₃, because the doublet corresponding to H_f is directly coupled to only one proton, H_d . H_d is directly coupled to the two H_i and is shifted downfield of its olefinic partner, H_f , as expected for a C=C-C=O system. Further supporting this conclusion, H_k protons were also shifted slightly for DDM-838 relative to DDM-840 as a result of the influence of the olefin, which provides evidence for conjugation with the carboxyl group. The identification of α -methyl serine was based in part on the observations that H_h protons are only split by each other, suggesting that they

are geminal protons in an oxazoline ring adjacent to a quaternary carbon. The acyl chain gave a typical terminal methyl triplet at 0.880 parts per million (ppm) and a large signal centered at 1.257 ppm, which obscures the signal from the methyl protons of the methyl serine associated with the oxazoline ring. Two obvious impurity peaks (6.97 and 3.775 ppm, upper panel), as well as spinning sidebands from the $CHCl_3$, have been deleted for clarity. Unassigned resonances, probably impurities, are denoted with an asterisk. Two-dimensional 1H - 1H data were also obtained and corroborate all implied adjacent proton relations (not shown). **(D)** This biosynthetic scheme is based on the previously proposed pathway of nonribosomal peptide synthesis (16, 20-22) and on the discovery of DDM as a dihydroxy form of mycobactin, which does not avidly bind iron. The DDM structure suggests that lysines are incorporated in the peptide, which is terminated by cyclization of the terminal lysine, acylated and hydroxylated on lysine residues as depicted (black arrows). This process would be an interesting variation of previously described siderophore biosyntheses in which amino hydroxylation occurs after acylation, and it remains possible that mycobactin could also be converted to DDM. The addition of hydroxamate moieties to the lysine residues adds two sites that participate in high-affinity interactions with ferric iron (Fe^{3+}), which facilitates the capture of iron from the host and subsequent transfer to the bacterium (16).

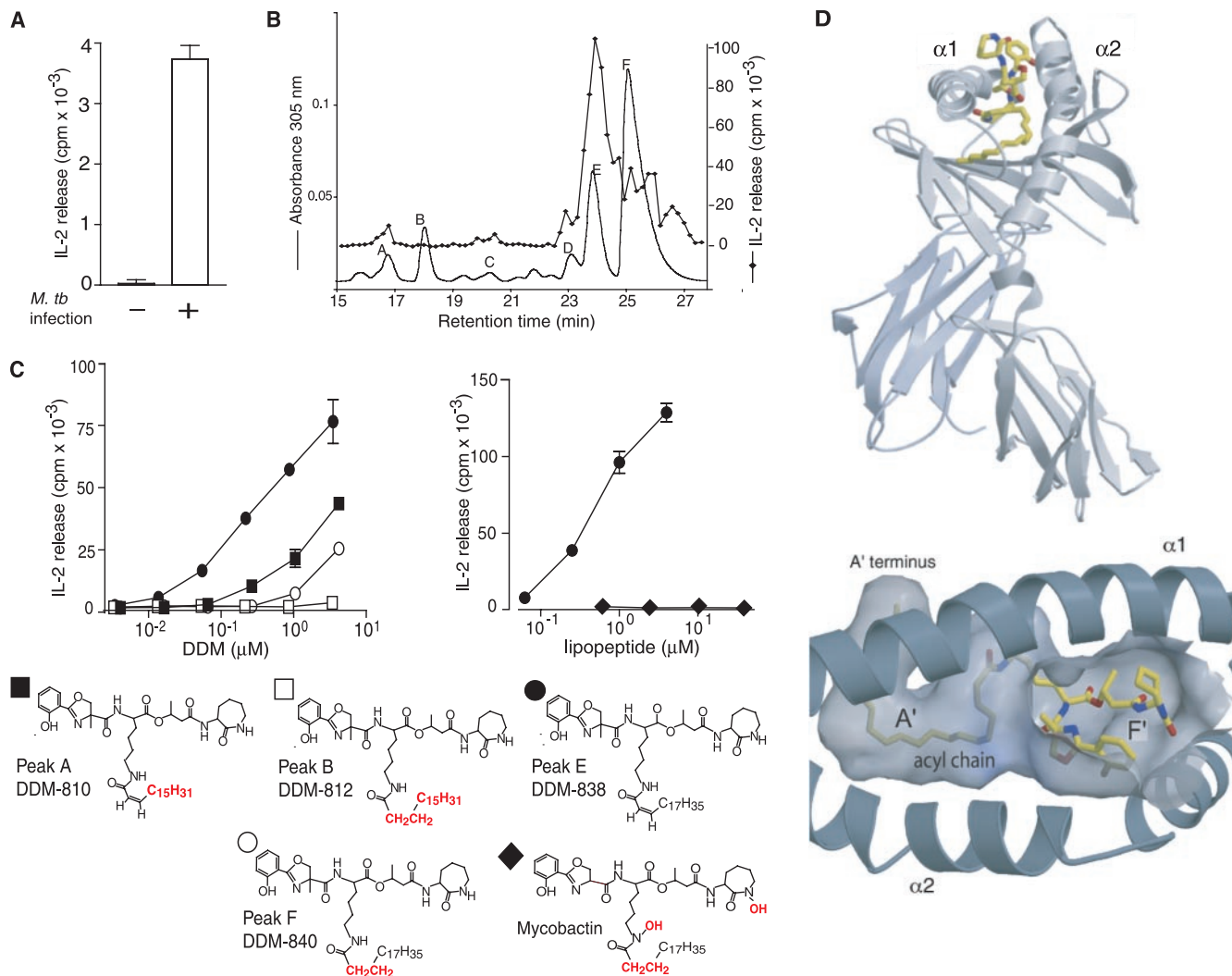


Fig. 3. The T cell response is specific for the structures of the lipid and peptide moieties of DDM-838. (A) IL-2 secretion by CD8-2/J.RT-3 above background levels found in resting JRT-3 cells was measured after coculture with monocyte-derived DCs that were infected with five bacteria per cell of *M. tuberculosis* H37Rv for 2 days. (B) After polar lipids from *M. tuberculosis* lipids were initially purified by precipitation in cold acetone and normal phase silica chromatography, an antigenic fraction containing DDM-838 was further resolved by HPLC on a C₁₈ column. Individual lipid species were detected by ultraviolet absorbance (solid line) and mass spectrometry (not shown). Fractions were collected at 15-s intervals, dried, resuspended in media, and tested for their ability to stimulate IL-2 release by J.RT3.CD8-2. (C) Lipids corresponding to peaks A, B, E, and F were subjected to further HPLC until resolved to homogeneity and examined by MS/MS. Compounds were named DDM-X, where X is the nominal mass of the [M+H]⁺ ion. MS/MS analysis demonstrat-

ed that material in peaks A, B, E, and F all yielded a product ion at *m/z* 546 (Fig. 2B), which indicates that the mass of the acyl chain, not the peptide, differed among these compounds, as shown in red. These compounds and mycobactin were tested for their ability to stimulate IL-2 release by J.RT3.CD8-2. (D) We prepared a molecular model of the CD1a-DDM complex using the programs MolScript and Raster3D after superimposing DDM-838 on the coordinates of CD1a (8, 34). The molecular surface of the CD1a binding pocket (bottom panel) was calculated in GRASP and is shown as a transparent gray surface that is predicted to interact with the carbon (yellow), nitrogen (blue), and oxygen (red) atoms of DDM (35). The volume and curvature of the hydrophobic CD1a groove correlate well with the size and shape of the optimal C20:1 (cis) acyl chain found in DDM-838, predicting that the peptidic portion of the antigen lies at the junction of the A' and F' pockets, near the α-helical surface of CD1a.

This model, along with the demonstrated role of TCR variable regions in antigen recognition (Figs. 1B and 3B), predict that the polypeptide backbone of the antigen serves as the contact for variable regions of the TCR, as is the case for conventional peptide antigens presented by MHC proteins (27, 28). Mammalian ribosomes translate DNA-encoded peptide sequences, which are post-translationally modified by acylation so that their structures resemble mycobacterial DDM but are highly varied in their peptide sequences (29). The autoreactivity of T cells for

CD1a proteins suggests that mammalian autoantigens bind to CD1a, and peptidases have been shown to regulate the recognition of CD1d presented antigens (4, 11, 30, 31). These observations raise the possibility that CD1 might also function to present structurally diverse lipopeptides encoded in the DNA of bacteria, viruses, or mammalian cells.

References and Notes

1. I. Mellman, R. M. Steinman, *Cell* **106**, 255 (2001).
2. S. Porcelli, C. T. Morita, M. B. Brenner, *Nature* **360**, 593 (1992).

3. E. Fithian *et al.*, *Proc. Natl. Acad. Sci. U.S.A.* **78**, 2541 (1981).
4. S. Porcelli *et al.*, *Nature* **341**, 447 (1989).
5. J. P. Rosat *et al.*, *J. Immunol.* **162**, 366 (1999).
6. A. Shamshiev *et al.*, *J. Exp. Med.* **195**, 1013 (2002).
7. Z. Zeng *et al.*, *Science* **277**, 339 (1997).
8. D. M. Zajonc, M. A. Elsliger, L. Teyton, I. A. Wilson, *Nature Immunol.* **4**, 808 (2003).
9. S. D. Gadola *et al.*, *Nature Immunol.* **3**, 721 (2002).
10. S. Stenger *et al.*, *Science* **276**, 1684 (1997).
11. M. S. Vincent *et al.*, *Nature Immunol.* **3**, 1163 (2002).
12. D. B. Moody *et al.*, unpublished observations.
13. E. M. Beckman *et al.*, *Nature* **372**, 691 (1994).
14. D. B. Moody *et al.*, *Science* **278**, 283 (1997).
15. D. B. Moody *et al.*, *Nature* **404**, 884 (2000).
16. G. A. Snow, *Bacteriol. Rev.* **34**, 99 (1970).

17. J. Gobin *et al.*, *Proc. Natl. Acad. Sci. U.S.A.* **92**, 5189 (1995).
 18. M. Tsukamoto *et al.*, *J. Antibiot. (Tokyo)* **50**, 815 (1997).
 19. A. F. Vergne, A. J. Walz, M. J. Miller, *Nat. Prod. Rep.* **17**, 99 (2000).
 20. S. T. Cole *et al.*, *Nature* **393**, 537 (1998).
 21. L. E. Quadri, J. Sello, T. A. Keating, P. H. Weinreb, C. T. Walsh, *Chem. Biol.* **5**, 631 (1998).
 22. J. J. De Voss, K. Rutter, B. G. Schroeder, C. E. Barry, *J. Bacteriol.* **181**, 4443 (1999).
 23. J. H. Crosa, C. T. Walsh, *Microbiol. Mol. Biol. Rev.* **66**, 223 (2002).
 24. O. Dussurget *et al.*, *J. Bacteriol.* **181**, 3402 (1999).
 25. J. De Voss *et al.*, *Proc. Natl. Acad. Sci. U.S.A.* **97**, 1252 (2000).
 26. S. Stenger, K. R. Niazi, R. L. Modlin, *J. Immunol.* **161**, 3582 (1998).
 27. D. N. Garboczi *et al.*, *Nature* **384**, 134 (1996).
 28. K. C. Garcia *et al.*, *Science* **274**, 209 (1996).
 29. P. J. Casey, *Science* **268**, 221 (1995).
 30. R. J. Riese *et al.*, *Immunity* **4**, 357 (1996).
 31. K. Honey *et al.*, *Nature Immunol.* **3**, 1069 (2002).
 32. D. B. Moody *et al.*, *Nature Immunol.* **3**, 435 (2002).
 33. E. P. Grant *et al.*, *J. Exp. Med.* **189**, 195 (1999).
 34. P. J. Kraulis, *J. Appl. Cryst.* **24**, 946 (1991).
 35. A. Nicholls, K. A. Sharp, B. Honig, *Proteins Struct. Funct. Genet.* **11**, 281 (1991).
 36. The authors acknowledge C. Ratledge for providing mycobactins and advice, C. A. Debono for bacterial culture, and J. Zajicek for preliminary NMR work. This work is supported by grants from the Ameri-

can College of Rheumatology Research and Education Foundation, the Cancer Research Institute, The Mizutani Foundation for Glycoscience, the Deutsche Forschungsgemeinschaft, and NIH or National Center for Research Resources grants (P20 RR16459 to S.B.L., AI50216 and AR48632 to D.B.M., GM62116 and CA58896 to I.A.W., AI30988 and GM25845 to M.J.M., and P41-RR10888 and S10-RR10493 to C.E.C.).

Supporting Online Material

www.sciencemag.org/cgi/content/full/303/5657/527/DC1

Materials and Methods Table S1

18 July 2003; accepted 20 November 2003

Role of LBPA and Alix in Multivesicular Liposome Formation and Endosome Organization

Hirokami Matsuo,^{1*} Julien Chevallier,¹ Nathalie Mayran,¹ Isabelle Le Blanc,¹ Charles Ferguson,³ Julien Fauré,⁴ Nathalie Sartori Blanc,⁵ Stefan Matile,² Jacques Dubochet,⁵ Rémy Sadoul,⁴ Robert G. Parton,³ Francis Vilbois,⁶ Jean Gruenberg^{1†}

What are the components that control the assembly of subcellular organelles in eukaryotic cells? Although membranes can clearly be distorted by cytosolic factors, very little is known about the intrinsic mechanisms that control the biogenesis, shape, and organization of organellar membranes. Here, we found that the unconventional phospholipid lysobisphosphatidic acid (LBPA) could induce the formation of multivesicular liposomes that resembled the multivesicular endosomes that exist where this lipid is found in vivo. This process depended on the same pH gradient that exists across endosome membranes in vivo and was selectively controlled by Alix. In turn, Alix regulated the organization of LBPA-containing endosomes in vivo.

Membranes and vesicles accumulate within multivesicular or multilamellar endosomes along the degradation pathway leading to lysosomes, and these selectively incorporate some proteins, including down-regulated receptors for growth factors and hormones (1, 2). In late endosomes, LBPA [or bis(monooacylglycerol)phosphate] is abundant in these internal membranes, accounting for ≈15 mole percent of total organelle phospholipids

(3). LBPA has not been detected elsewhere in the cell and is involved in protein and lipid trafficking through late endosomes (3–7).

We synthesized 2,2'-dioleoyl LBPA (8) (Fig. 1, A and B), the major isoform (>90%) in baby hamster kidney (BHK) cells (9), and we prepared large liposomes (10) with a phospholipid composition similar to that of late endosomes (dioleoylphosphatidylcholine: dioleoylphosphatidylethanolamine: phosphatidylinositol:LBPA, 5:2:1:2 mol) (3, 9). When labeled with the fluorescent dye FM2-10, large unilamellar liposomes (diameters of ≈600 to 800 nm) were easily revealed by light microscopy, whether LBPA was present (Fig. 1C) or not present (Table 1). Because the late endosomal lumen is acidic (pH 5.0 to 5.5) (1), we mimicked this situation in vitro by incubating lipids at pH 5.5 during the phase reversion of the liposome assembly process; the external pH was then neutralized to reproduce the pH gradient formed in vivo (10). Liposomes lacking LBPA remained unilamellar (Fig. 1D and Table 1), whereas LBPA liposomes showed 5 to 10 internal vesicles (Fig. 1E and Table 1), thus resembling multivesicular regions of the late endosomes that were observed by electron microscopy (EM) (3, 9, 11, 12). Internal vesicles were also observed within LBPA-

Table 1. MVLs. Liposomes were prepared at pH 5.5 or 7.4, or they were prepared at pH 7.4 and then the internal pH was switched to pH 5.5 (10). After labeling with FM 2-10, an aliquot of the assay mixture was mounted onto a coverslip (final volume = 3 μl), and the number (n) of MVLs was counted (10). About 300 liposomes from three independent experiments were counted for each condition. Data are also expressed as a percentage (%) of the number of MVLs in the presence of 2,2'-LBPA and a pH gradient. pH in, liposome pH; pH out, external pH; aLBPA Ab, antibody to LBPA; IC AB, isotypic control antibody. ND, not determined.

	pH in/pH out = 5.5/7.4		pH in/pH out = 7.4/7.4	
	n	%	n	%
<i>Liposomes prepared at pH 5.5 or pH 7.4</i>				
2,2'-dioleoyl LBPA	91	100	2	2
Control (no LBPA)	4	4	3	3
2,2'-dioleoyl LBPA + aLBPA Ab	4	4	ND	ND
2,2'-dioleoyl LBPA + IC AB	74	81	ND	ND
3,3'-dioleoyl LBPA	17	19	3	3
3,3'-dimyristoyl LBPA	2	2	4	4
Trimyristoyl semi-LBPA	1	1	1	1
Trioleoyl semi-LBPA	4	4	1	1
<i>Liposomes prepared at pH 7.4 and then switched to pH 5.5</i>				
2,2'-dioleoyl LBPA	107	100	ND	ND
Control (no LBPA)	15	14	ND	ND
2,2'-dioleoyl LBPA + aLBPA Ab	10	10	ND	ND
2,2'-dioleoyl LBPA + IC AB	64	60	ND	ND

¹Department of Biochemistry, ²Department of Organic Chemistry, University of Geneva, 30 quai Ernest Ansermet, 1211 Geneva 4, Switzerland. ³Institute for Molecular Bioscience, Center for Microscopy and Microanalysis and School of Biomedical Sciences, University of Queensland, Queensland 4072, Australia. ⁴Neurodégénérescence et Plasticité Inserm–Université Joseph Fourier, Hôpital A. Michallon, 38043 Grenoble Cedex 9, France. ⁵Laboratoire d'Analyse Ultrastructurale, University of Lausanne, 1015 Lausanne, Switzerland. ⁶Serono Pharmaceutical Research Institute, 1228 Plan-les-Ouates, Switzerland.

*Present address: Department of Chemical Pharmacy, Shujitsu University, 1-6-1 Nishigawara, Okayama 703-8516, Japan.

†To whom correspondence should be addressed. E-mail: jean.gruenberg@biochem.unige.ch